Zeszyty Naukowe WWSI, No 22, Vol. 14, 2020, pp. 23-38
DOI: 10.26348/znwwsi.22.23

Application of artificial neural networks in preliminary selection of pigmented lesions for further melanoma diagnosis

Anna Kisielińska-Ptasznik*and Ewa Figielska†

Warsaw School of Computer Science

Abstract

The paper deals with the problem of preliminary selection of pigmented lesions for further melanoma diagnosis. Several algorithms for input data pre-processing are proposed and artificial neural network for the examination of pigmented lesions is used. Computational results are reported.

***Keywords* —** Artificial neural network, Data pre-processing, Melanoma diagnosis

1 Introduction

The aim of the paper is the examination of the possible use of artificial neural networks in preliminary selection of pigmented lesions for further melanoma diagnosis. Data sets used for melanoma diagnosis usually contain pigmented lesions photos which were taken by different devices, in different lighting conditions and in different resolutions. Therefore, the application of artificial neural networks for unprocessed and non-standard input data is not possible. In the paper, some image pre-processing algorithms for the extraction and standardisation of selected features of pigmented lesions are proposed. The computer system is developed in which the image pre-processing algorithms are used for the preparation of training and test data sets for an artificial neural network. The neural network is implemented with the use of ML.NET library. The results of computational experiments are presented and the designed system is evaluated.

2 Melanoma issue description

2.1 What is melanoma?

Melanoma is cancer, usually concerning skin, which arises from melanocytes, i.e. the cells producing melanin [1]. It can develop as a new lesion on the skin or as a change in the existing

*E-mail: a_kisielinska@poczta.wwsi.edu.pl
†E-mail: efigielska@poczta.wwsi.edu.pl

Manuscript received July 11, 2020

pigmented lesion (change in thickness, surface, colour or borders) [2]. The following stages can be identified taking into account the transformation of benign lesion into malignant melanoma:

- atypical lesion (pre-malignant neoplasm) constituting the basis for melanoma development,
- primary melanoma in radial growth phase, where melanoma cells spread horizontally, penetrating epidermis,
- primary melanoma in vertical growth phase, where melanoma cells spread vertically penetrating subsequent skin layers and can have metastatic capacity,
- malignant melanoma, causing metastases.

In the case of the majority of neoplasms, the processes responsible for developing metastatic capacity and malignancy by cancer cells may last for many years, however, in the case of melanoma it happens in much shorter time, which can be just a few months. Furthermore, small tumours at the initial stages of development (I or II stage) hardly ever form metastases. Therefore, early diagnosis of melanoma is the key factor increasing the chance for survival, as its successful treatment consists mainly in surgery, before it develops metastatic capacity. Additional treatment including chemotherapy, radiotherapy or immunotherapy is employed only when justified, however, their effectiveness is quite poor.

Even though melanoma is not the most frequent skin cancer as it constitutes only $5-7\%$ of the cases, it actually causes 80% of deaths of skin cancer. Statistics show that 91% of patients with melanoma have a chance for 5-year survival since the diagnosis and removal of the primary tumour, though it should be diagnosed at early stage (tumour thickness less than 1 mm). With the appearance of metastases, 5-year survival rate decreases to 15% [1].

2.2 Diagnosing melanoma

The most popular and recommended examination used in preliminary diagnostics is dermoscopy (dermatoscopy) or videodermoscopy. The most important principle is examination of all the lesions existing on the skin, not only those of suspicious appearance, in order to eliminate the possibility of overlooking an early stage of melanoma. There are several methods for dermoscopic analysis, we will focus on one of them called the ABCDE method.

ABC system standing for Asymmetry, Border irregularity, Colour variegation was introduced in 1985 by the team of New York University in response to the need for education of doctors and society in the identification of early stages of melanoma. Moreover, the members of New York University School of Medicine Melanoma Cooperative Group, basing on their experience with patients, came to the conclusion that asymmetry, border irregularity and colour variegation of the early stage melanoma were associated with the diameter more than 6 mm., thus the three criteria were complemented by the fourth – D (Diameter). In the meantime, also the importance of changes in lesion appearance was confirmed as a significant melanoma feature, which resulted in addition of E standing for Evolution to ABCD acronym. ABCDE system was meant to be simple, universal, directed at identification of early melanoma stages, therefore many features characteristic of advanced stages (e.g. ulcerative lesions) are excluded

from the analysis. The suitability of ABCDE criteria was verified in clinical studies, their effectiveness was confirmed also in the analysis of digital images. Nowadays, these criteria are used worldwide, as simple features enabling the identification of pigmented lesions requiring further diagnostics [3].

The criteria of the ABCDE system are described in detail below [2]:

- A (Asymmetry) – melanoma is asymmetric with reference to each axis, while benign lesions are usually round or oval,
- B (Borders) – borders are uneven and jagged,
- C (Colour) – colour is diversified (from light brown to black or steel) with uneven distribution of pigment,
- D (Diameter) – the diameter is more than 5 mm or the (Dynamics) dynamics of morphological changes in the tumour can be identified,
- E (Elevation or Evolution) – there is elevation of the lesion surface above the level of epidermis surrounding the lesion. Thin melanomas ($\leq 1mm$) do not form palpable lump in comparison with normal skin surrounding the lesion; however, diameter extension (Extension or Evolution) is much more important than the lesion elevation.

The described above criteria are assessed with regard to their compliance with expectations (e.g. lack of asymmetry, asymmetry with reference to one axis, asymmetry with reference to two axes). The higher are the deviations, the more points are assigned to a given category, as a result of which the sum of all the points allows the calculation of Total Dermatoscopy Score (TDS) indicator, whose value is used to determine if the examined lesion is melanotic or benign [4]. It should be stressed that not every melanoma case meets all ABCDE criteria. The lesion may arouse suspicion of early melanoma stage based on co-occurrence of two or more parameters (e.g. ABC, $A + C$) [3].

As a result of dermoscopic examination, the suspicious lesion is qualified for dissection and histopathological evaluation of the whole dissected lesion. If melanoma is diagnosed, it undergoes staging, according to which proper treatment is chosen. The most commonly applied classification is Tumour, Node, Metastasis (TNM) scale determined in 2010 by American Joint Committee on Cancer (AJCC). Thanks to the application of this scale, the most important information of a given melanoma case can be gathered including the size of the tumour, the presence of cancer cells in lymph nodes and the metastases located in distant areas of the body [1].

3 Image pre-processing

The problem we encounter when trying to use a neural network for the preliminary selection of pigmented lesions is a huge number of images required for its training. This is caused by different sources of images, differences in quality, lighting and gradation, different types of image noise (dirt, dust, hair on the picture) and so on. This problem can be solved, and thus the size of a training set reduced, by the extraction and digitalisation of several features of images.

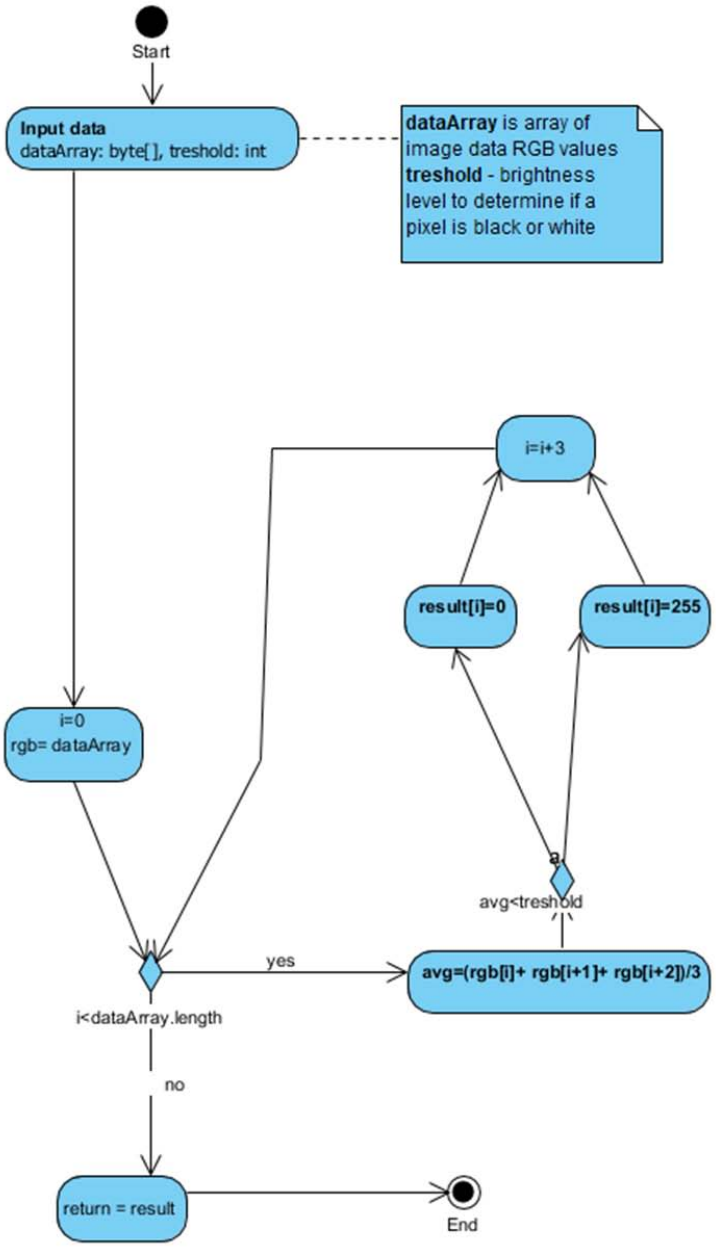

Figure 1: Algorithm for 24-bit colour image conversion to black and white one

Figure 2: Original image of lesion (a) and the results of black and white processing with threshold levels: 45 (b), 130 (c) and 220 (d).

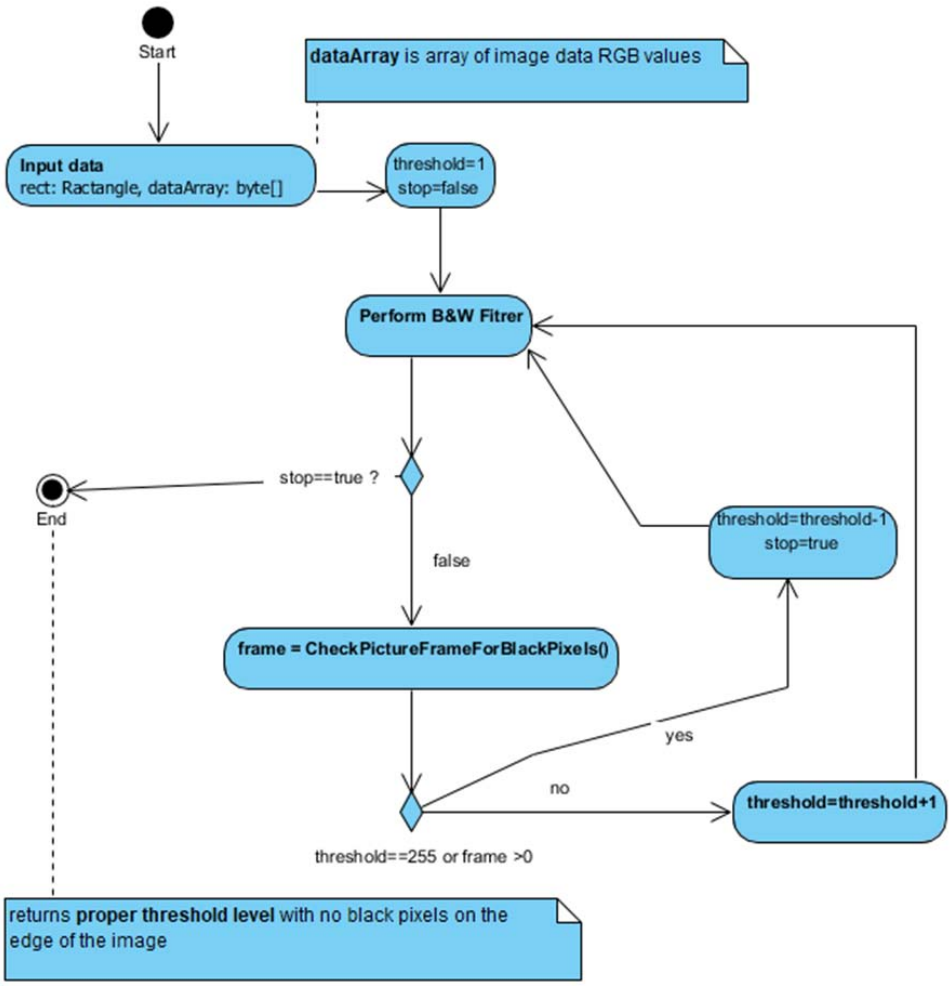

Figure 3: Algorithm for proper threshold value detection

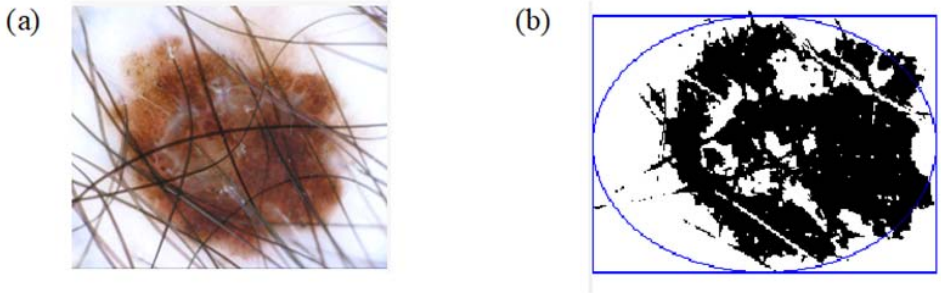

Figure 4: Lesion with the noise in the form of hair: the original image (a), the image transformed with the black-white filter – unsuccessful transformation (b)

3.1 Shape extraction

The first task indispensable for other tasks completion is localisation of the lesion on the image and its shape extraction. Subsequent tasks, like border or asymmetry analysis, require knowledge of localisation and finding the potential symmetry centre. As a rule, lesions are darker than surrounding skin and they can be distinguished by means of black and white filter.

Black and white filter transforms colour image e.g. with 24-bit colour depth into monochromatic bitmap, where colour depth is 1-bit, by reading RGB values of each pixel, calculating the average of RGB values and comparing the average with threshold value. Averaged value denotes the brightness of the pixel, therefore the value under the threshold is represented by black pixel and the value over the threshold is represented by white pixel. The algorithm described above is depicted in Figure 1.

Nevertheless, the problem occurs while determining threshold level with regard to the fact that the photos can be taken in different lighting conditions, with various skin tones. Thus, it cannot be constant value. An experiment was conducted on sample images of lesions (taken from the website of the ISIC – International Skin Imaging Collaboration [5]) during the filter development (Figure 2). While experimenting with black and white filter by changing threshold value from minimum to maximum (the range: $0 - 255$), it was observed that the lesion on the picture visualized as a black spot, step by step started to resemble the original lesion shape (Figures 2b and 2c). Further increase in the threshold value resulted in appearance of black pixels also outside the lesion shape (Figure 2d) and finally they covered the whole image.

On the basis of these observations, the algorithm was developed in order to detect proper threshold value for each image. Difficulty consisted in determining the moment, when threshold level exceeds the average brightness of remaining part of the skin and white background of the lesion starts to cover with black pixels. The concept of the algorithm is based on the examination if the background area covers with black pixels while increasing the threshold level. Image edges are the area, which with the highest probability can be the background of the lesion, thus they are used in the algorithm. Considering the image edges, a certain margin (of $5 - 10$ pixels) should be assumed, as examination of appearance of black pixels on the one-pixel edge did not

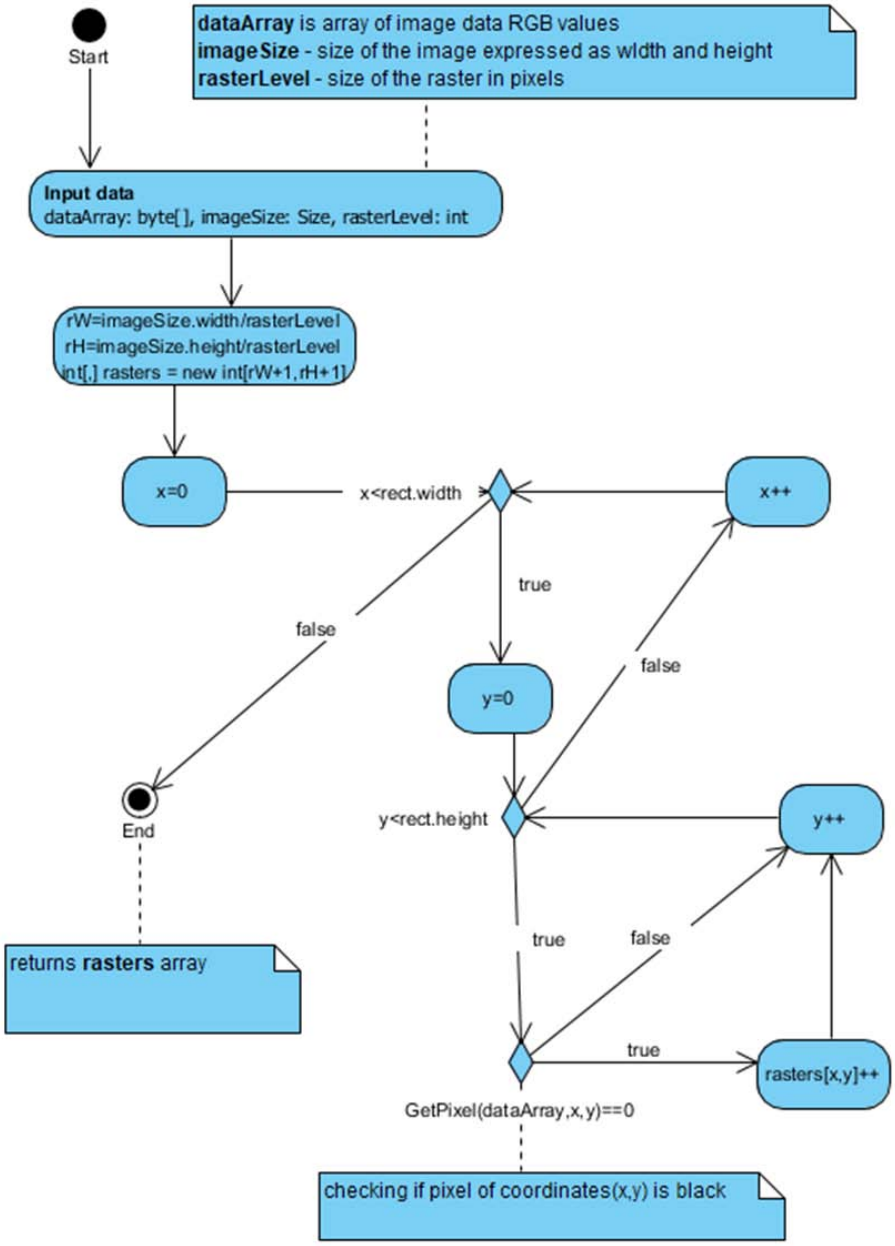

Figure 5: Algorithm for image rasterization

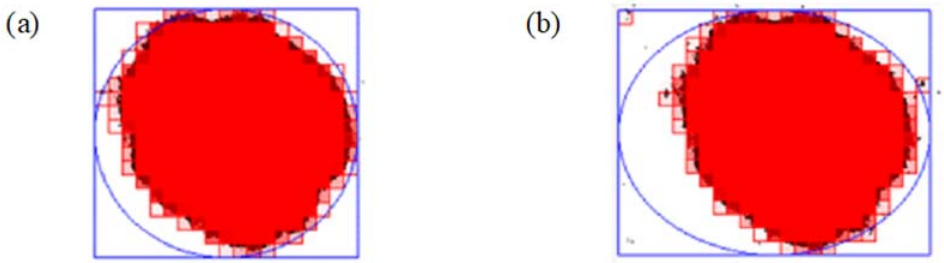

Figure 6: Rasterization of black and white image with threshold value equal to 197 (a) and 204 (b)

give a positive result. The algorithm is presented in Figure 3.

As it was mentioned above, the noise often appears on the images, so manipulation on single pixels was not effective and caused the algorithm to stop too early. Figure 4 presents the image of the lesion, on which noise in the form of hair appeared (Figure 4a) and an unsuccessful attempt of border threshold value detection (Figure 4b). It can be clearly observed that black hair prevented correct detection of the lesion shape. The algorithm stopped with too low value of threshold level as a result of the detection of black pixel on the edge and the lesion was not correctly mapped.

Therefore, the mechanism of averaging parts of the image was designed in order to eliminate the possibility of interrupting the algorithm operation by single pixels. It divides the image into rasters (squares with specified side) and calculates the number of black pixels in each raster, which makes it possible to define approximate area of the lesion (rectangle or ellipse inscribed into rectangle) and its potential symmetry centre. The algorithm for rasterization is depicted in Figure 5.

Figure 6 presents the images of the lesion transformed into black and white form with division into rasters. Rasters are presented as squares with red edge and filled with red colour, the transparency of which depended on the number of detected black pixels. In Figure 6a, the division into rasters was made after transformation of the original image into black and white form with the threshold value of 197. In Figure 6b, the threshold value of 204 was used. The resulting image contains at least 5 pixels in the left upper corner, so this area was detected as a raster. This resulted in inaccurate setting of the size and localisation of the lesion as well as incorrect calculation of its symmetry centre.

Due to the rasterization mechanism it is possible to identify that threshold value reached the level of background brightness and the algorithm should be stopped. Searching the rasters rather than single pixels eliminates a part of measurement errors resulting from different kinds of noise on the image. The algorithm for the proper threshold value detection using rasterization is presented in Figure 7.

The application of the algorithm shown in Figure 7 leads to elimination of single pixels not only on the edge of the image but also in the whole rasters due to which the lesion shape can be properly determined. Figure 8a shows the sample image of the lesion, in Figure 8b the

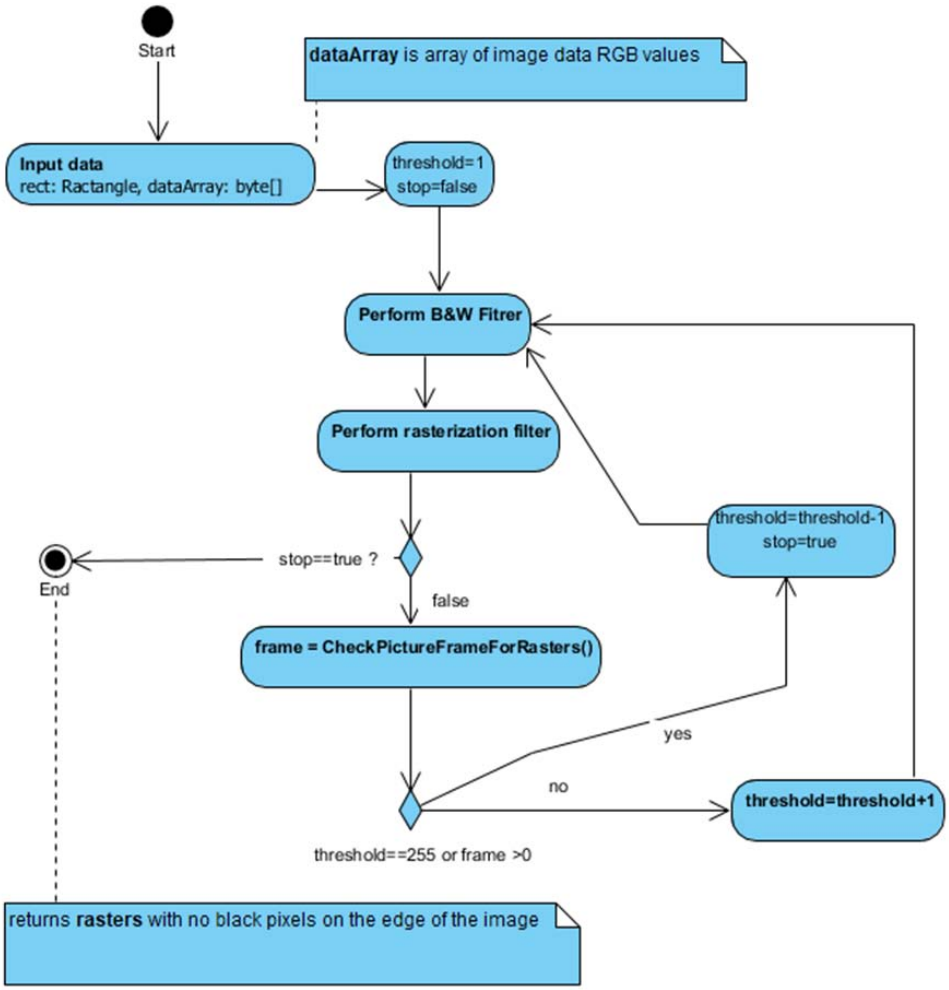

Figure 7: Algorithm for the proper threshold value detection using rasterization

transformed and rasterized lesion is presented. Two pixels near the left edge of the image were detected (light red rectangle) but still they were not taken into account in the calculation of lesion size.

3.2 Border analysis

The concept of examining the border irregularity is based on the determination of the lesion potential symmetry centre as well as the detection of the length of polar radiuses determined by the most distant black pixels on the subsequent radiuses (Figure 9).

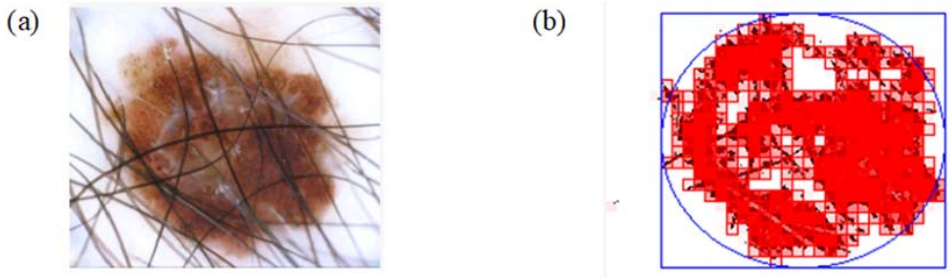

Figure 8: Original image of the lesion (a) and transformed and rasterized lesion with the noise ignored (b)

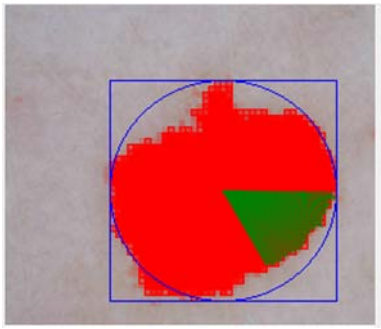

Figure 9: Radiuses detection during processing

Ideally, when the lesion is in the shape of a circle, all radiuses are equal. When the edge is irregular, the differences between the subsequent radiuses appear. The irregularity of edges can be determined as the normalized sum of squares of the differences in the lengths of successive radiuses and is given by the following formula:

$$Border = \frac{1}{360M} \sum_{i=0}^{359} (B_{i+1} - B_i)^2 , \tag{1}$$

where B_i denotes the ith radius, $M = \max_{0 \leq i < 360} B_i$. Using the squares of differences in the radius lengths is necessary because lesions may have ellipse shape with regular edges which otherwise could be defined as irregular. For such lesions the differences between successive radiuses occur but they are relatively small in comparison with the differences for lesions with irregular edges. The irregularity is normalised, as it should be independent of the lesion size.

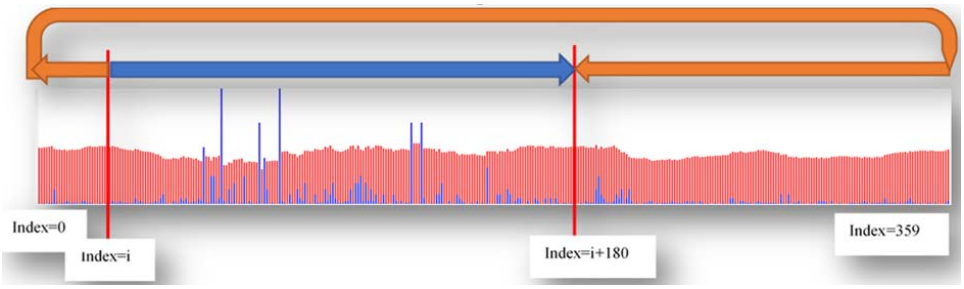

Figure 10: Asymmetry analysis concept

3.3 Asymmetry analysis

The next challenge is the investigation of the lesion asymmetry. In connection with the fact that it is unknown where the symmetry axis runs, all the possibilities should be investigated (with a specified precision). The proposed solution is based on the division of the array B containing radius lengths into two parts.

More precisely, first, two arrays R_i and L_i ($i = 0, \cdots, 179$) are constructed so that array R_i contains values of radius lengths from positions from i to $i + 179$ in B, and array L_i contains radiuses from positions from 0 to $i - 1$ and from $i + 180$ to 359 in B. The idea of division of the set into two parts is presented in Figure 10.

Then, arrays R_i and L_i are compared. Before examining the difference between subsequent radiuses from both arrays, the order of the elements of one of them is reversed. As a symmetry measure, denoted by S_i, we take the sum of absolute diffrences between corresponding radiuses from both parts:

$$S_i = \sum_{k=0}^{179} |R_i[k] - L_i[k]| \,. \tag{2}$$

We introduce the measure of the lesion asymmetry A expressed by the following equation:

$$A = \min_{0 \le i < 180} S_i. \tag{3}$$

For lesions of symmetrical shape, such i can be found for which $S_i = 0$. For asymmetrical lesions, we expect S_i to be greater than 0 for each i.

3.4 Colour analysis

The analysis of the lesion colour in terms of its differentiation requires statistical approach. Additionally, in connection with high colour depth of the analysed images equalling to 24 bits i.e. about 16.7 million colours as well as the noise, which always occurs on photos, it is justified to average the colour and reduce colour depth.

The developed algorithm, presented in Figure 11, creates colour histogram and returns the number of averaged colours occurring on the image. For each pixel, from detected earlier

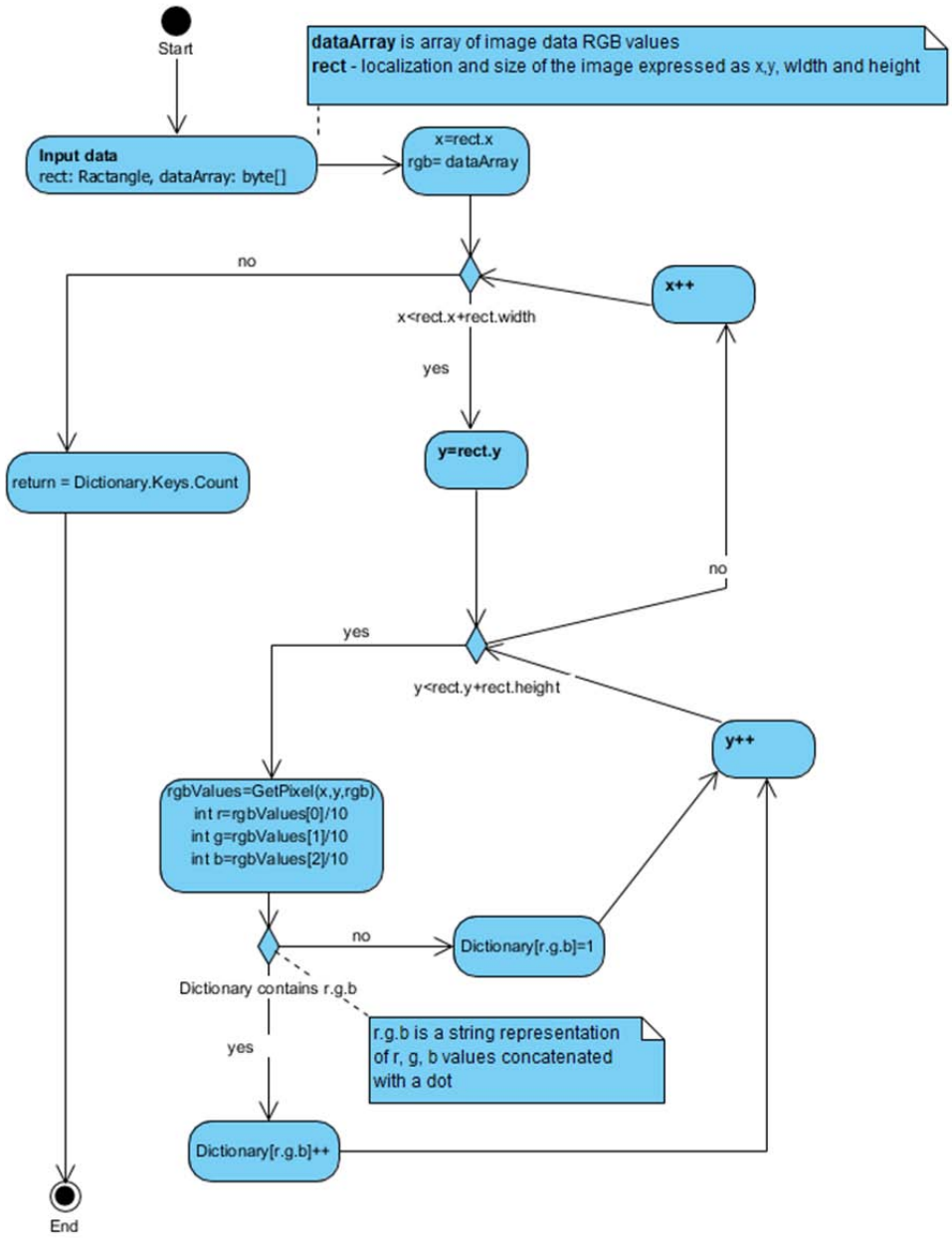

Figure 11: Algorithm for colour differentiation recognition

```
Asymetry,Border,Color,Melanoma
1985,0.720332986472422,214,1
633,0.478475765306122,264,1
1347,0.551436901291128,136,1
2417,0.949588477366256,99,1
722,0.151104899991266,374,1
3229,1.03878981862521,441,1
3651,2.06593132154006,452,1
1330,0.46791647614693,191,1
1017,0.0609288119664814,397,1
```

Figure 12: Training data set - excerpt from the data file.

lesion area, the colour is read by RGB components. Subsequently, each component is averaged by dividing its value by 10 using floor function. The certain representation is created for each ordered RGB set and its occurrence is calculated in colour histogram. Representation of RGB sets can be in the form of a string of characters composed of the RGB components values connected by dot.

The proposed approach entails a certain risk of error, since the analysed area comprises both the lesion and the surrounding skin, however, in connection with the fact that each image will be analysed this way, the ratio of colour differentiation will be adequate for only the colouring of the lesion. In order to improve the adequacy of this approach, earlier calculations and data used for the investigation of lesion shape can be applied.

4 System

The application called "MelanomaProject" was written in $C\#$ with the use of Visual Studio Community 2017 [6]. For the implementation of neural network examining if extracted ABC features are melanoma specific or not, ML.NET library is used. The library enables the configuration of the model, carrying out model training and evaluation. ML.NET makes available several mechanisms and machine learning algorithms. In order to use ML.NET functions for loading data to the model, input data should be prepared in csv (Comma-separated values) format. The main module of "MelanomaProject" application enables saving ABC features from pre-processed images in the form of csv file. Excerpt from the file with training data is shown in Figure 12. Its first line includes data labels and subsequent lines include ABC data (separated by commas) extracted from particular images of training dataset as well as the information on diagnosis.

The main window of the system is shown in Figure 13. The functionalities of the system are presented in Table 1.

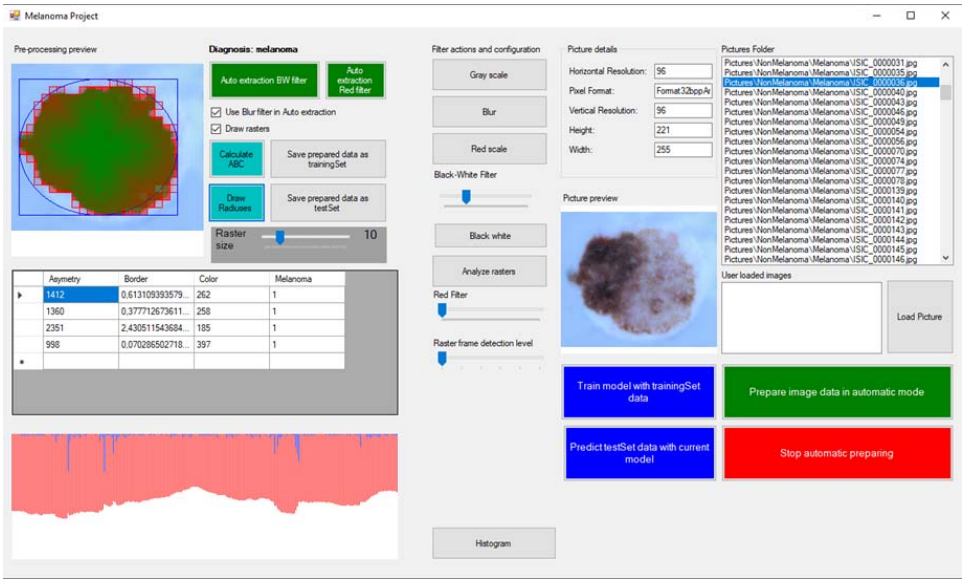

Figure 13: Main window of ”MelanomaApplication”

Table 1: Functional specification of the program

#	**Functionality**
1	Loading and displaying images of pigmented lesions, loading JSON files with metadata including diagnosis and additional information on the patient
2	Processing the image by means of black white filter with the possibility of setting threshold level
3	Processing the image by means of rasterization with the possibility of setting raster size
4	Drawing the detected lesion area
5	Detecting and drawing radiuses
6	Calculating ABC indicators for the selected image: detecting radiuses' lengths, lesion asymmetry and lesion colour variegation
7	Displaying diagnosis for the selected image, if metadata file is available
8	Displaying calculated ABC indicators for processed images in tabular form with the possibility of manual diagnosis setting (in case of the lack of metadata file)
9	Automatic processing of images collection: calculating and displaying ABC indicators
10	Saving ABC indicators to the format accepted by neural network as a training set and as testing set
11	Running neural network training
12	Running neural network testing for the images uploaded by the user

5 Experiments

Several experiments and tests were carried out, the aim of which was to explore the possibility of the application of neural networks in the identification of melanotic lesions. After developing the application, preceded by series of tests verifying the correctness of implemented algorithms, the training of neural network prepared in ML.NET based on Averaged Perceptron algorithm was carried out (averaged perceptron training algorithm corresponds with single-layer neural network). For the training process, training dataset was prepared that consisted of 214 images loaded from the website of the ISIC [5] along with the information on diagnosis. The dataset underwent pre-processing and was saved in csv file. Next, the model was trained and saved, and subsequently it was evaluated by determining its average accuracy (accuracy is the number of correctly classified items divided by the total number of items). The evaluation was made by means of a cross-validation with 5 folds.

In the experiment, the average accuracy of 0.712 was obtained with standard deviation and confidence interval equal to, respectively, 0.064 and 0.063 (at significance level of 0.05).

It seems that the incorrect responses are caused by the following factors:

1. Lesion edges are too close or beyond image frame; in such case, lesion size detection algorithm stopped too early.
2. Too small number of images in training process.
3. Too small number of features extracted from the image – greater number of features would probably make it possible for the neural network to find more accurate correlation of input data with the expected result, unless these features did not have a major impact on the diagnosis. In such case the neural network could perform even worse.

In practice, confirming the neoplasm diagnosis is far more important for the patient and the doctor than ruling it out, as such decision entails entirely different consequences and actions. Ruling out the neoplasm would probably result in suggesting that patient should have a follow-up appointment, while confirming melanoma diagnosis would result in necessity of lesion dissection and its histopathological evaluation or additional diagnostics. Therefore, two additional metrics are employed: average positive precision (the number of positive instances predicted as positive, divided by the total number of instances predicted as positive) and average negative precision (the number of negative instances predicted as negative, divided by the total number of instances predicted as negative). As the result we obtained the values of the average positive precision and average negative precision equal to 0.739 and 0.702, respectively, which means that the precision of the neoplasm prediction is higher than the precision of the benign lesion prediction.

The subsequent experiment was carried out using about 100 cases that were obtained from images of good quality (e.g. without noise) which were properly featured during pre-processing. Half of the cases represented melanoma data and the second half – non-melanoma data. The obtained results are as follows: average accuracy $= 0.794$ (standard deviation $= 0.086$, confidence interval $= 0.085$), average positive precision $= 0.820$ and average negative precision $= 0.781$. The precision of prediction increased in both cases (positive and negative precision), together with the averaged accuracy. It can be concluded that training data quality is far more

important than its quantity, and thanks to this quality, the model can achieve better learning outcomes.

6 Final remarks

Within the accomplishment of the objectives the paper, the concept and the application were developed which use contemporary tools of machine learning in the process of diagnosing melanoma. Even though, nowadays there are a lot of useful tools or libraries implementing more and more advanced algorithms of machine learning, still data quality and the understanding of problem domain is crucial for effectiveness of even the most advanced tool. If only it is possible, the algorithms should be developed and data pre-processing should be carried out, so that neural network could successfully learn and make predictions.

References

[1] M. Janik, D. Hoja-Łukowicz, S. D. Szajda, N. Waszkiewicz, and M. Przybyło, "Czerniak: najbardziej złośliwy nowotwór skóry," in *Zapobieganie chorobom nowotworowym*, S. D. Szajda, N. Waszkiewicz, K. Zwierz, and J. R. Ładny, Eds. Wyższa Szkoła Zawodowa Ochrony Zdrowia Towarzystwa Wiedzy Powszechnej, 2016, pp. 87–109.

[2] P. Rutkowski, P. J. Wysocki, A. Nasierowska-Guttmejer, J. Fijuth, E. Kalinka-Warzocha, T. Świtaj, A. Jeziorski, M. Szacht, W. Zegarski, W. M. Wysocki *et al.*, "Cutaneous melanoma—diagnostic and therapeutic guidelines in 2016," *Oncology in Clinical Practice*, vol. 11, no. 4, pp. 216–231, 2015.

[3] D. S. Rigel, J. Russak, and R. Friedman, "Ewolucja w diagnostyce czerniaka złośliwego: 25 lat po wprowadzeniu kryteriów ABCD," *Onkologia po Dyplomie*, vol. 8, no. 3, pp. 49–68, 2011. [Online]. Available: https://podyplomie.pl/publish/system/articles/pdfarticles/000/014/122/original/49-68.pdf

[4] M. Hałat-Łaś. Diagnostyka znamion barwnikowych. [Online]. Available: https://biotechnologia.pl/kosmetologia/diagnostyka-znamion-barwnikowych,13844

[5] ISIC Gallery. [Online]. Available: https://www.isic-archive.com/#!/topWithHeader/onlyHeaderTop/gallery

[6] A. Kisielińska-Ptasznik, "Application of artificial neural networks in preliminary selection of pigmented lesions for further melanoma diagnosis," Master thesis, Warsaw School of Computer Science, 2019.